4U1700+24: a puzzling symbiotic

Nucita A.A., Masetti N. Stefanelli S., ,Manni L, De Paolis, F., Del Santo M.

Department of Mathematics and Physics "Ennio de Giorgi", University of Salento, and INFN (sez. Lecce), via per Arnesano CP-193, 73100, Lecce (Italy)
INAF – Istituto di Astrofisica Spaziale e Fisica Cosmica di Bologna, via Gobetti 101, I-40129 Bologna, Italy
INAF/IAPS, via del Fosso del Cavaliere, 100, I-00133, Roma, Italy

Symbiotic X-ray binaries form a subclass of low-mass X-ray binary systems consisting of a neutron star accreting material from a red giant donor star via stellar wind or Roche lobe overflow. Only a few confirmed members are currently known; 4U 1700+24 is a good candidate as it is a relatively bright X-ray object, possibly associated with the late-type star V934 Her We analysed the archive XMM-Newton and Swift/XRT observations of 4U 1700+24 in order to have a uniform high-energy (0.3 – 10 keV) view of the source. Apart from the 2003, 2010, and 2012 data, publicly available but still unpublished, we also took the opportunity to re-analyze a set of XMM-Newton data acquired in 2002. Methods. After reducing the XMM-Newton and Swift/XRT data with standard methods, we performed a detailed spectral and timing analysis. We confirmed the existence of a red-shifted O VIII Ly- transition (already observed in the 2002 XMM-Newton data) in the high-resolution spectra collected via the RGS instruments. The red-shift of the line is found I all the analysed observations and, on average, it was estimated to be ≃ 0.009. We also observed a modulation of the centroid energy of the line on short time scales (a few days) and discuss the observations in the framework of different scenarios. If the modulation is due to the gravitational red-shift of the neutron star, it might arise from a sudden re-organization of the emitting X-ray matter on the scale f a few hundreds of km. Alternatively, we are witnessing a uni-polar jet of matter (with typical velocity of 1000–4000 km s−1) possibly emitted by the neutron star in an almost face-on system. The second possibility seems to be required by the apparent lack of any modulation in the observed X-ray light curve. We also note also that the low-resolution spectra (both XMM-Newton and Swift/XRT in the 0.3–10 keV band) show the existence of a black body radiation emitted by a region (possibly associated with the neutron star polar cap) with typical size from a few tens to hundreds of meters.

Symbiotic stars?

Symbiotic X-ray binaries (SyXBs) form a tiny subclass of Galactic low-mass X-ray binaries (LMXBs) characterized by a red giant star (generally of spectral type M) which loses matter to a compact object, most likely a neutron star (NS), via stellar wind, or (less frequently, as in the case of GX 1+4; Chakrabarty & Roche 1997) Roche lobe overflow. Only seven confirmed members are currently known, while for other candidates like 1RXS J180431.1-273932 (Nucita et al. 2007) follow-up observations allowed us to exclude the SyXB nature (see Masetti et al. 2012 and references therein). However, according to stellar population synthesis studies performed by Lü et al. (2012), between 100 and 1000 of these objects are expected to be in the Galaxy (although one should note that half of the SyXBs considered by the authors were found to be either spurious or unconfirmed cases).

The SyXB subclass only started gaining some attention from the scientific community in the last decade only; however, X-ray studies of these sources are still quite sporadic, with only a handful of objects having been explored in this spectral window (Masetti et al. 2002, 2007a,b, Rea et al. 2005, Paul et al. 2005, Tiengo et al. 2005, Mattana et al. 2006, Patel et al. 2007, Corbet et al. 2008, Marcu et al. 2011, González-Gallan et al. 2012).

ONE OF THESE SOURCES IS 4U 1700+24

X-ray spectroscopy of the source, obtained over the last decades (Garcia et al. 1983, Dal Fiume et al. 1990, Masetti et al. 2002), shows a continuum typical of accreting LMXBs, with a thermal component probably originating on or near the accretor and a Comptonized emission detected up to 100 keV. In particular, Masetti et al. (2002) examined the X-ray spectroscopic properties of the source using data collected with several satellites over 13 years, from 1985 to 1998. After this study, Tiengo et al. (2005) published a paper on the X-ray behaviour of 4U 1700+24: the authors analysed an observation collected with the *XMM*-Newton satellite in 2002 and found an emission feature at ≈ 0.5 keV and an emission line at ≃ 0.64 keV which was possibly identified as the red-shifted O VIII Ly-α transition.

No further investigations on the X-ray spectroscopic behaviour of 4U 1700+24 have been performed since then; however, three more *XMM*-Newton pointings performed in 2003 and seven Swift/XRT observations made in 2010 and 2012 are publicly available but still unpublished.

For your info

Table 1. Log of the archive *XMM*-Newton observations analysed in this paper.

OBS. ID	REV	NOM. RA (deg)	NOM. DEC (deg)	POS. ANGLE (deg)	DATE (yr-m-d)	START (h:m:s)	END (h:m:s)	NOM.DUR. (ks)	EXP. TIME (ks)
0155960601 *	489	256.64370	23.97183	295.63034	2002-08-11	15:55:49.0	19:32:02.0	13	–, –, 3.2
0151240301 *	593	256.64385	23.97183	79.403876	2003-03-07	01:08:08.0	04:32:20.0	12	–, –, 1.3
0151240201 *	594	256.64385	23.97183	79.399512	2003-03-09	01:03:49.0	04:27:57.0	12	–, –, 5.5
0151240401	673	256.64385	23.97183	294.30723	2003-08-13	15:23:12.0	19:40:38.0	15	9.4, 9.2, 7.8

Note: The observations labelled with an asterisk presented pile-up in the EPIC cameras. We were able to correct for the pile-up only the EPIC pn data. Hence, in these cases, we avoided using the MOS 1 and MOS 2 events in order to prevent spurious effects (see text for details); as a consequence, a symbol – appears in the last column.

Table 2. Log of the archive Swift/XRT observations analysed in this paper.

OBS. ID	DATE (yr-m-d)	START (h:m:s)	END (h:m:s)	EXP. TIME (ks)
0009080001	2010-05-30	20:29:06	23:39:56	1.4
0009080002	2010-06-04	12:55:00	00:16:58	9.7
0054025500 *	2012-12-02	05:07:33	13:12:24	12.8
0054025501 *	2012-12-02	13:13:56	23:14:27	6.4
0054025502 *	2012-12-03	14:56:26	23:03:44	5.3
0054025503 *	2012-12-04	00:47:17	10:28:36	5.8
0054025504 *	2012-12-05	13:21:41	18:11:36	5.9

Note: The observations labeled with an asterisk presented pile-up.

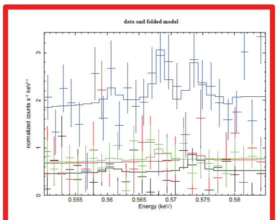

Fig. 3. A zoom around the O VII triplet (data points rebinned in order to have a signal-to-noise ratio of 5 in each bin) and the best-fit model superimposed after red-shifting the rest-frame energy of the complex by $\Delta\lambda/\lambda \simeq 0.009$, i.e. the energy found when analyzing the O VIII Ly-α.

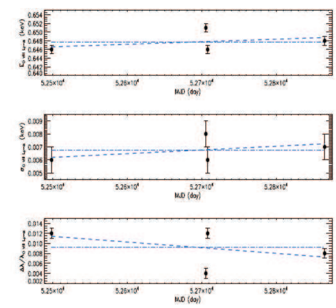

Fig. 2. Here, we show the centroid position in keV (upper panel) as determined by the Gaussian line fit, the line width (middle panel), and the red-shift factor of the O VIII Ly-α line identified in the high-resolution spectra of 4U1700+24 as a function of the observation time (defined as the average time of each exposure) in modified Julian date. In each panel, the dot-dashed line represents a fit with a constant, while the dashed line accounts for any linear trend possibly associated with the data (see text for details).

A redshifted O VIII Ly-a is identified without any ambiguity once the OVII complex is found where it is expected to be! The line position evolves with time.

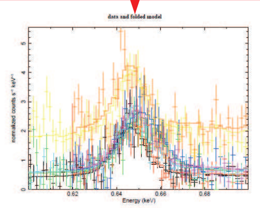

Fig. 1. A zoom of the RGS 1 and 2 spectra of 4U1700+24 around the O VIII Ly-α emission line (at about ≃ 19 Å) for all the observations quoted in Table 1. The spectra were binned in order to have a signal-to-noise ratio of 5 in each bin, and we give the horizontal axis in energy instead of wavelength. The data in yellow/orange (corresponding to the 2002 observation, i.e. 0155960601) clearly show a large continuum component with respect to the other data sets, thus reflecting the high activity of the source at that time. The solid lines represent the best-fit model as described in the text.

Table 3. For each of the *XMM*-Newton observations, we give the main best-fit parameters (normalization, centroid position energy E_{obs}, line width σ_{obs}, and wavelength λ_{obs}) of the emission feature observed at ≃ 19 Å (see text for details).

OBS. ID	MJD (day)	N_2 ($cm^{-2}s^{-1}$)	E_{obs} (keV)	σ_{obs} (keV)	λ_{obs} (Å)	$\Delta\lambda/\lambda$	v km s^{-1}
0155960601	52498.21	$(9.0 \pm 1.0) \times 10^{-4}$	$0.646^{+0.001}_{-0.001}$	$0.006^{+0.001}_{-0.001}$	$19.195^{+0.030}_{-0.030}$	$0.012^{+0.001}_{-0.002}$	3600^{+300}_{-600}
0151240301	52705.58	$(1.1 \pm 0.2) \times 10^{-3}$	$0.651^{+0.001}_{-0.001}$	$0.008^{+0.001}_{-0.001}$	$19.048^{+0.030}_{-0.030}$	$0.004^{+0.002}_{-0.002}$	1200^{+600}_{-600}
0151240201	52707.99	$(8.4 \pm 1.0) \times 10^{-4}$	$0.646^{+0.001}_{-0.001}$	$0.006^{+0.001}_{-0.001}$	$19.195^{+0.030}_{-0.030}$	$0.012^{+0.002}_{-0.002}$	3600^{+600}_{-600}
0151240401	52865.22	$(9.9 \pm 1.0) \times 10^{-4}$	$0.648^{+0.001}_{-0.001}$	$0.007^{+0.001}_{-0.001}$	$19.136^{+0.030}_{-0.030}$	$0.009^{+0.001}_{-0.002}$	2400^{+300}_{-600}

SO WHAT?

A red-shift of the O VIII Ly-α line in the range $0.002 - 0.013$ (see the estimated values given in Table 3) can be explained (see also Tiengo et al. 2005) as the gravitational red-shift of the photons emitted by a plasma blob at distance R from an object with mass M, i.e. $\Delta\lambda/\lambda = 1/(g_{00})^{0.5} - 1$ with $g_{00} = 1 - 2GM/Rc^2$. As can be seen, the possibility that 4U 1700+24 hosts a white dwarf can easily be ruled out because, for the typical values of white dwarf mass and radius ($M \simeq 1$ $M_\odot$ and $R \simeq 2 \times 10^4$ km), the expected gravitational red-shift is a factor of 10 (or more) lower than the observed value. In agreement with Garcia et al. (1983), this supports the idea that 4U 1700+24 is a neutron star that accretes matter from a red giant. Assuming a neutron star mass of ≃ 1.4 $M_\odot$ in the 4U 1700+24 binary system, the detected red-shift range corresponds to the gravitational red-shift of a photon emitted at a distance of 160 − 1000 km from the central object, i.e. consistent with the value found by Tiengo et al. (2005) when analyzing the 2002 *XMM*-Newton observation. Furthermore, a close inspection of Fig. 2 allows us to conclude that the red-shift of the O VII Ly-α line is variable on a time scale of few days (see the log of the observations in Table 1). In particular, the red-shifts estimated for the central observations 0151240301 and 0151240201 are ≃ 0.004 and ≃ 0.012, respectively. Since these estimates differ from the average red-shift value by more than $3 - 5\sigma$, we are confident that the effect is real. Excluding Doppler contributions due to the orbital motion of any blob of plasma around the neutron star (as the associated signatures would be different to the observations presented here), we conclude that we are witnessing the re-organization of matter at a distance of a few hundred kms around the accreting object. An alternative picture would be a jet of matter (with typical velocity of 1000 − 4000 km s^{-1}) possibly emitted away by the neutron star in an almost face-on system. The alternative condition seems to be required by the apparent lack of any periodicity and/or modulation (as we have verified via a Lomb-Scargle analysis) in the observed *X*-ray light curve. However, as also observed by Tiengo et al. (2005), the puzzling lack of any blue-shifted component implies the necessity of an ad-hoc geometry to explain the observations or one could invoke a uni-polar jet emitted by the neutron star.

Table 4. The best fit model describing the EPIC data (first four rows) and Swift/XRT data (last seven rows) consists in an absorbed black body plus a Comptonization to which two emission lines (at ≃ 0.5 keV and ≃ 0.6 keV) were added (see text for details).

ObsID	kT_{BB} (keV)	N_{BB} R^2_{km}/D^2_{10}	kT_c (keV)	τ	N_C $Nf/4\pi D^2$	E_1 (keV)	σ_1 (keV)	N_1 ($cm^{-2}s^{-1}$)	N_2 ($cm^{-2}s^{-1}$)
0155960601	$0.90^{+0.09}_{-0.06}$	$9.00^{+1.16}_{-2.33}$	$2.11^{+0.08}_{-0.06}$	$34.56^{+0.93}_{-2.20}$	$0.0183^{+0.0007}_{-0.0004}$	$0.464^{+0.028}_{-0.011}$	$0.131^{+0.009}_{-0.024}$	$0.017^{+0.001}_{-0.003}$	≤ 0.0004
0151240301	$0.82^{+0.07}_{-0.03}$	$6.94^{+1.76}_{-1.39}$	$2.12^{+0.20}_{-0.09}$	$27.93^{+2.68}_{-2.68}$	$0.0072^{+0.0005}_{-0.0006}$	$0.485^{+0.020}_{-0.028}$	$0.093^{+0.035}_{-0.024}$	$0.005^{+0.002}_{-0.001}$	$0.0007^{+0.0005}_{-0.0004}$
0151240201	$1.13^{+0.10}_{-0.10}$	$2.66^{+0.24}_{-0.26}$	$2.45^{+0.45}_{-0.22}$	$24.00^{+1.88}_{-3.60}$	$0.0071^{+0.0003}_{-0.0002}$	$0.490^{+0.012}_{-0.011}$	$0.043^{+0.014}_{-0.012}$	$0.0019^{+0.0004}_{-0.0004}$	$0.0010^{+0.0001}_{-0.0001}$
0151240401	$0.71^{+0.05}_{-0.05}$	$6.98^{+2.25}_{-1.41}$	$1.96^{+0.05}_{-0.05}$	$33.07^{+1.88}_{-1.27}$	$0.0075^{+0.0002}_{-0.0004}$	$0.487^{+0.008}_{-0.022}$	$0.108^{+0.018}_{-0.010}$	$0.007^{+0.001}_{-0.001}$	$0.0007^{+0.0001}_{-0.0003}$
0009080001	$1.02^{+0.11}_{-0.08}$	$0.50^{+0.10}_{-0.10}$	(2.16)	$16.29^{+3.44}_{-2.89}$	$0.0008^{+0.0001}_{-0.0001}$	–	–	–	$0.0003^{+0.0001}_{-0.0001}$
0009080002									
0054025500	$0.89^{+0.19}_{-0.13}$	$5.02^{+3.20}_{-1.96}$	(2.16)	$28.96^{+2.88}_{-3.10}$	$0.0070^{+0.0008}_{-0.0009}$	–	–	–	$0.0012^{+0.0005}_{-0.0005}$
0054025501	$1.05^{+0.28}_{-0.23}$	$2.3^{+2.0}_{-1.0}$	(2.16)	$27.34^{+5.34}_{-9.70}$	$0.0040^{+0.0008}_{-0.0005}$	–	–	–	$0.0009^{+0.0005}_{-0.0001}$
0054025502	$0.77^{+0.17}_{-0.10}$	$5.6^{+4.1}_{-2.6}$	(2.16)	$32.58^{+7.90}_{-4.90}$	$0.0031^{+0.0008}_{-0.0005}$	–	–	–	$0.0011^{+0.0005}_{-0.0005}$
0054025503	$0.98^{+0.30}_{-0.16}$	$4.7^{+3.5}_{-1.9}$	(2.16)	$31.94^{+9.30}_{-3.90}$	$0.004^{+0.001}_{-0.001}$	–	–	–	$0.0013^{+0.0006}_{-0.0006}$
0054025504	$0.88^{+0.29}_{-0.17}$	$1.4^{+1.4}_{-0.7}$	(2.16)	$28.90^{+4.28}_{-4.80}$	$0.0020^{+0.0003}_{-0.0003}$	–	–	–	$0.0011^{+0.0003}_{-0.0003}$

Hint: the polar cap decreases as the luminosity goes down

Table 5. The $0.3 - 2$ keV, $2 - 10$ keV and $0.3 - 10$ keV band fluxes together with the estimated luminosity (full band) for a source distance of ≃ 420 pc.

ObsID	MJD (day)	$F_{0.3-2.0kev}$ (10^{-10} erg cm^{-2} s^{-1})	$F_{2-10.0kev}$ (10^{-10} erg cm^{-2} s^{-1})	$F_{0.3-10.0kev}$ (10^{-10} erg cm^{-2} s^{-1})	$L_{0.3-10.0kev}$ (10^{34} erg s^{-1})
0155960601	52498.22	$0.669^{+0.006}_{-0.021}$	$4.35^{+0.02}_{-0.12}$	$5.02^{+0.03}_{-0.17}$	$1.060^{+0.010}_{-0.040}$
0151240301	52705.58	$0.290^{+0.005}_{-0.021}$	$1.23^{+0.02}_{-0.19}$	$1.52^{+0.03}_{-0.16}$	$0.320^{+0.010}_{-0.040}$
0151240201	52707.99	$0.245^{+0.005}_{-0.004}$	$1.25^{+0.01}_{-0.09}$	$1.49^{+0.01}_{-0.08}$	$0.310^{+0.002}_{-0.020}$
0151240401	52865.22	$0.284^{+0.002}_{-0.004}$	$1.41^{+0.01}_{-0.03}$	$1.69^{+0.01}_{-0.04}$	$0.355^{+0.002}_{-0.010}$
0009080001	55346.92	$0.031^{+0.014}_{-0.008}$	$0.080^{+0.015}_{-0.007}$	$0.110^{+0.020}_{-0.010}$	$0.023^{+0.013}_{-0.006}$
0009080002	55351.78				
0054025500	56263.38	$0.246^{+0.007}_{-0.020}$	$1.30^{+0.06}_{-0.10}$	$1.54^{+0.06}_{-0.13}$	$0.324^{+0.013}_{-0.027}$
0054025501	56263.76	$0.145^{+0.006}_{-0.016}$	$0.773^{+0.093}_{-0.146}$	$0.920^{+0.180}_{-0.160}$	$0.193^{+0.038}_{-0.034}$
0054025502	56264.79	$0.143^{+0.005}_{-0.016}$	$0.739^{+0.045}_{-0.142}$	$0.880^{+0.110}_{-0.160}$	$0.185^{+0.023}_{-0.034}$
0054025503	56265.23	$0.186^{+0.007}_{-0.037}$	$1.09^{+0.08}_{-0.22}$	$1.27^{+0.10}_{-0.27}$	$0.267^{+0.021}_{-0.057}$
0054025504	56266.66	$0.077^{+0.003}_{-0.012}$	$0.373^{+0.029}_{-0.086}$	$0.450^{+0.030}_{-0.093}$	$0.095^{+0.006}_{-0.020}$

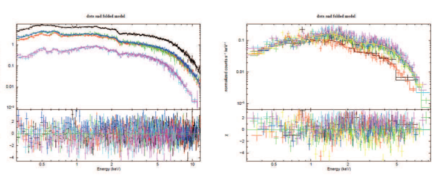

Fig. 4. Left panel: the EPIC spectra of 4U1700+24 during the four observations analysed in this work. Black, green, blue, and red data points correspond to the EPIC pn data of the observations 0155960601, 0151240301, 0151240201, and 0151240401, respectively. Since the pile-up affected most of the data sets, MOS 1 and MOS 2 data (purple and cyan data points) were only available for the last observation (i.e. 0151240401). Here, the solid lines correspond to the best-fit model described in the text. Right panel: the Swift/XRT spectra of 4U1700+24 during the 2010 and 2012 observations (data points) together with the best-fit model (solid lines). Here, the black and red data correspond to the Swift observations 0009080001 and 0009080002, respectively while the other data sets shown (purple, blue, yellow, green and cyan) correspond to the observation IDs from 0054025500 to 0054025504 of Table 4.

Based on these facts, we prefer a scenario in which the mass coming from the M-type companion stellar wind (see Postnov et al. 2011 and references therein for details on the wind accretion in symbiotic *X*-ray binaries) is captured directly onto a small zone of the NS surface. The *X*-ray photons emitted are reprocessed by a blob of matter at a few hundred kms from the NS surface so that the output emission features are gravitationally red-shifted.

Main References for a first look

Nucita A. A., et al., 2014, A&A, 783, 86 (and references therein)
Tiengo et al., et al., 2005, 441, 283

Contacts: nucita@le.infn.it, luigi.manni@le.infn.it